Patterned Self-Assembled Monolayers on Silicon Oxide Prepared by Nanoimprint Lithography and Their Applications in Nanofabrication**

Pascale Maury, Mária Péter, Venkataramanan Mahalingam, David N. Reinhoudt, and *Jurriaan Huskens**

Nanoimprint lithography (NIL) is used as a tool to pattern self-assembled monolayers (SAMs) on silicon substrates because of its ability to pattern in the micrometer and nanometer ranges. The polymer template behaves as a physical barrier preventing the formation of a SAM in the covered areas of the substrate. After polymer removal, SAM patterns are obtained. The versatility of the method is shown in various nanofabrication schemes. Substrates are functionalized with a second type of silane adsorbate. Pattern enhancement via selective electrostatic attachment of carboxylate-functionalized particles is achieved. Further applications of the NIL-patterned substrates include template-directed adsorption of particles, as well as the fabrication of electrodes on top of a SAM.

1. Introduction

Creating patterns of self-assembled monolayers (SAMs) using top–down and bottom–up approaches is receiving increasing interest. Such methods allow one to chemically pattern a substrate, opening new possibilities for etch resists[1,2] or to control the position and attachment of molecules and particles with different functionalities on a substrate. Different applications have been demonstrated for patterned, functionalized SAMs. For instance, the use of functionalized molecules has made it possible to fabricate sensors[3] and molecular electronic devices.[4,5] Working with proteins, biological arrays can be prepared[6] and, employing (non-functionalized) nanoparticles, photonic crystals can be fabricated.[7–9] Controlling the functionality of the chemical pattern allows one to build up complex systems.[10] The end-group functionality of a patterned SAM can, for example, be used to direct the assembly of functionalized nanoparticles. Positioning of functionalized particles can be used in chemistry to study specific interactions between

SAM and nanoparticle interfaces on patterned substrates, in biology for sensors, and in physics for photonic crystals as well as for data storage. Specific attachment of functionalized particles has already been studied, but typically on micrometer-scale patterns and employing micrometer-sized particles.[11,12] Also, the deposition of non-functionalized particles has been studied, again using micrometer-scale patterns.[13]

Several methods exist to pattern SAMs, the most well known being microcontact printing[14] and dip-pen nanolithography,[15] which employ the transfer of an ink to the substrate. Classical top–down techniques, such as electron-beam lithography (EBL) and photolithography, have also been used, either by employing a polymer template[16] or by local modification of the end-group functionality of the SAM upon irradiation.[17] These top–down methods have been mainly used for silanes on silicon oxide because it is difficult to pattern silanes using microcontact printing. This difficulty arises because of the tendency of silanes to polymerize in the presence of water from the environment. The combination of EBL and gas-phase silanation gives good results, but EBL is time-consuming and expensive. Therefore, in our work we chose to use another soft-lithography technique to pattern silane-based SAMs, namely, nanoimprint lithography (NIL).[18]

In NIL, a hard stamp (e.g., a patterned Si wafer) is pressed against a substrate covered with a thin layer of polymer. First, the sample and stamp are heated above the glass-transition temperature (T_g) of the polymer and then pressure is applied. After cooling the system to below the T_g of the polymer, the pressure is released and the stamp is removed. Features of the stamp are thus transferred into the polymer. A thin, residual layer of polymer remains and this can be removed in an etching step. This method allows patterning in three dimensions, with feature sizes down to 6 nm.[19] Using this technique, designs of rather arbitrary shape and aspect ratios of up to five can be molded into the polymer by choosing appropriate experimental conditions (such as temperature, pressure, and imprint time). The resolution of NIL is limited by the stamp resolution and by

DOI: 10.1002/adfm.200400284
© 2005 WILEY-VCH Verlag GmbH & Co. KGaA, Weinheim **451**

FULL PAPER

the polymer properties when imprinting features below 10 nm. This technique is characterized by its high resolution, low cost, and high throughput.[20] It has been widely used in physics for electronic and photonic applications,[21,22] in biology,[23] and, to a lesser degree, in chemistry.[24]
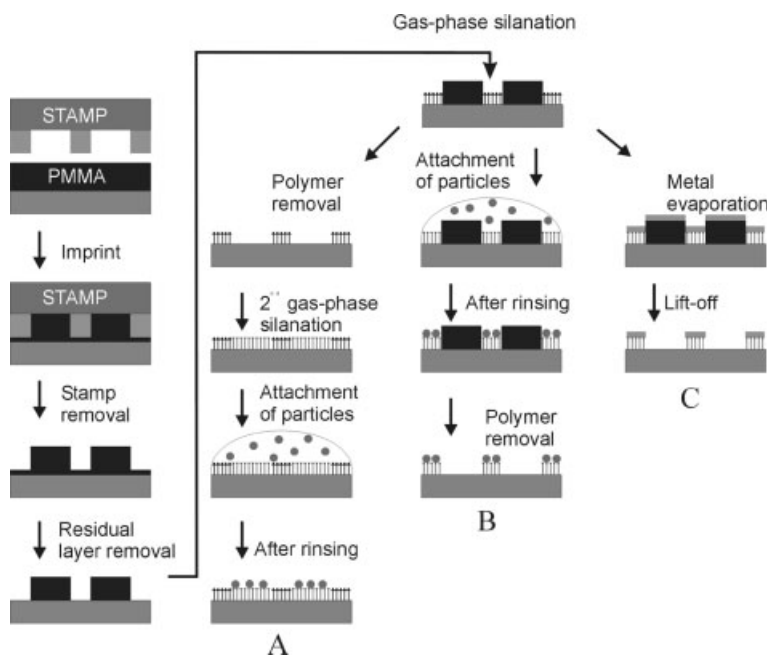
Here, we describe the use of NIL to prepare patterned SAMs of silanes on SiO_2. The polymer pattern is used as a mask to evaporate a silane from the gas phase onto the uncovered regions. The polymer is removed and, if necessary, a second gas-phase silanation with a different silane can be performed. An advantage of using NIL is that the polymer template allows multi-step processing. The end-group functionality of the patterned SAM is used to direct the deposition of functionalized particles, both on samples where the polymer patterns are still maintained to employ them as a physical barrier for particle deposition, and on samples where the polymer patterns have been removed and a second silane has been adsorbed to tune the selectivity of the adsorption process. In this paper, initial results are shown using micrometer- and sub-micrometer-sized patterns, using functionalized particles (polystyrene and silica) with dimensions of down to 50 nm. Metal evaporation followed by metal lift-off has also been performed to show the possibility of further applications in molecular electronics. These processes are summarized in Scheme 1.

Scheme 1. Schematic representations of the NIL process and of three applications after SAM patterning. A) Evaporation of a second type of silane after mask removal and attachment of functionalized particles. B) Attachment of functionalized particles using the polymer template, followed by polymer removal. C) Metal evaporation followed by metal lift-off.

2. Results and Discussion

### 2.1. Monolayer Patterning Using NIL

A 400 nm thick layer of poly(methyl methacrylate (PMMA, weight-average molecular weight, M_W: 350 kD) was deposited on silicon oxide substrates by spin-coating (see Scheme 1, left column). NIL was performed at a pressure of 40 bar and a temperature of 180 °C. The residual layer was removed either by O_2-plasma etching or by dipping the samples in acetone for 60 s. Figure 1 shows atomic force microscopy (AFM) images of a NIL-patterned substrate before and after residual-layer removal by dipping in acetone for 60 s. The height profile shows a decrease of the full width at half maximum (FWHM) of about 800–600 nm, consistent with the isotropic polymer dissolution process. The Figure shows, however, that the imprinted lines after residual-layer removal are still rectilinear and that the linewidths of the exposed areas after residual-layer removal are comparable to the spacing between the tops of the polymer patterns before residual-layer removal,[25] which can also be obtained by anisotropic etching.

The residual layer was removed in acetone because dry etching, which is the usual method to remove the residual layer, can cause damage to the substrate.[26] In an O_2-plasma process, even for an exposure of only few seconds, bombardment by O_2 ions can slightly modify the height of the exposed silicon as
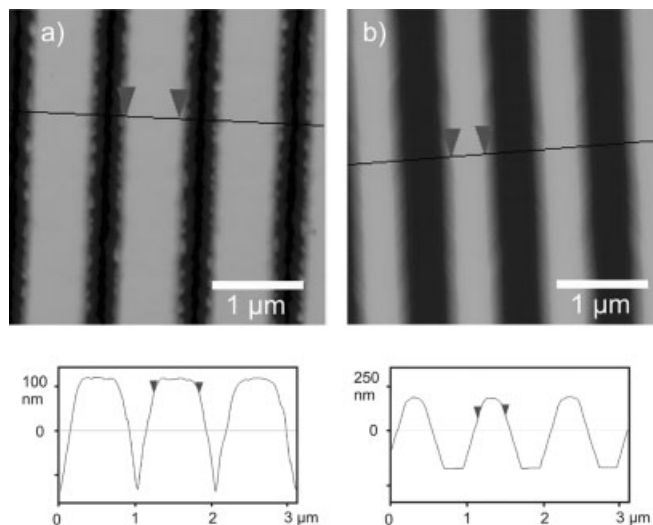
Figure 1. Contact-mode height AFM images of an imprint a) before and b) after residual-layer removal by dipping the imprint in acetone for 60 s. The marks on the cross-section of the height images indicate a width of 600 nm.

well as increase the hydrophilic nature of the substrate.[27] For example, structures with a typical height of 1.5 nm were found after O_2-plasma etching, and some contrast in the AFM friction images could be seen. Therefore, AFM studies of SAM formation on the exposed parts of the imprinted substrates would be difficult to analyze when using plasma etching. AFM

images of a NIL-patterned sample after residual-layer removal in acetone, followed by complete polymer removal showed differences neither in height nor in friction. An X-ray photoelectron spectroscopy (XPS) spectrum of the same sample showed a clean silicon substrate with a very low carbon content, identical to a blank unprocessed silicon wafer cleaned in piranha solution (see Experimental). Therefore, this proves that the polymer can be completely removed and that our method for removal of the residual layer did not lead to surface changes of the substrate.

Imprints were performed on PMMA deposited on silicon substrates treated with piranha solution in order to produce an oxidized surface necessary for the covalent attachment of the silanes. Different kinds of silanes, with CF_3-, NH_2-, Br-, and CH_3-terminated groups, respectively, were deposited to modify the outer surface of the NIL-patterned substrates. The polymer left after imprinting and removal of the residual layer acts as a mask for gas-phase evaporation of the silane adsorbates. Gas-phase deposition is used to avoid damage to the polymer, e.g., by swelling in a solvent. Finally, the polymer was removed in acetone using ultrasound.

Figure 2 shows AFM images of an array of fluoroalkyl SAM lines of 5 μm width at a 15 μm period (Figs. 2a,b) and aminoalkyl SAM lines of 400 nm width at a 1 μm period (Figs. 2c,d). The SAMs have formed on the complementary areas of the NIL patterns. The quality of the patterned SAM was found to be the same as on non-patterned SAM blanks. The measured height of the patterned layer, when investigating large patterns (5 μm lines), was found to correspond to the

height of a monolayer. In the case of small patterns, such as Figure 2c, the height was hard to measure accurately, probably due to contamination of the sample. In the case of the NH_2-terminated monolayer, a higher friction force was observed relative to the substrate (Fig. 2d), in agreement with the hydrophilic nature of this silane adsorbate. In contrast, for the hydrophobic monolayers such as CF_3-terminated SAMs (Fig. 2b), and CH_3- and Br-terminated monolayers (not shown), lower friction forces were observed relative to the substrate (Table 1).

Table 1. Advancing (θ_{adv}) and receding (θ_{rec}) water contact angles on unpatterned SAMs, monolayer thickness measured using contact-mode AFM, and relative friction forces on patterned SAMs. Patterned samples were prepared by forming a SAM on a NIL-patterned substrate, followed by polymer removal.

Adsorbates	$\theta_{adv}/\theta_{rec}$ [deg/deg]	Height [nm]	Friction force
N-[3-(trimethoxysilyl)propyl]ethylenediamine	65/20	0.8	High
dodecyltrichlorosilane	109/89	0.7	Low
bromoundecyltrichlorosilane	101/83	0.7	Low
1*H*,1*H*,2*H*,2*H*-perfluorodecyltrichlorosilane	117/76	3.4	Low

The resolution of the patterning process was further investigated using NIL stamps containing lines and dots with dimensions down to 150 and 125 nm, respectively, made by EBL and metal lift-off. Figure 3 shows AFM height (Figs. 3a,c) and fric-
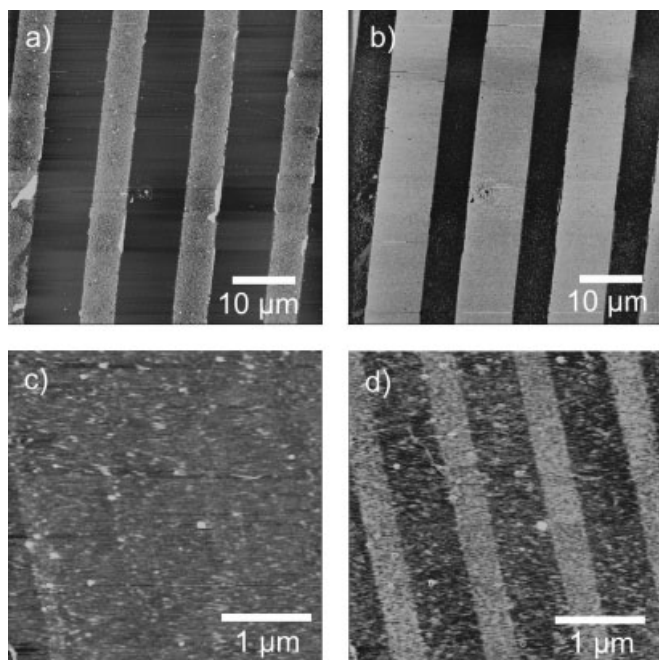
Figure 2. Contact-mode height (a,c) and friction (b,d) AFM images of 5 μm fluoroalkyl SAM lines at a 15 μm period (a,b) and of 400 nm aminoalkyl SAM lines at 1 μm period (c,d) on NIL patterned substrates followed by SAM formation and polymer removal. In the friction images, brighter areas indicate higher friction.
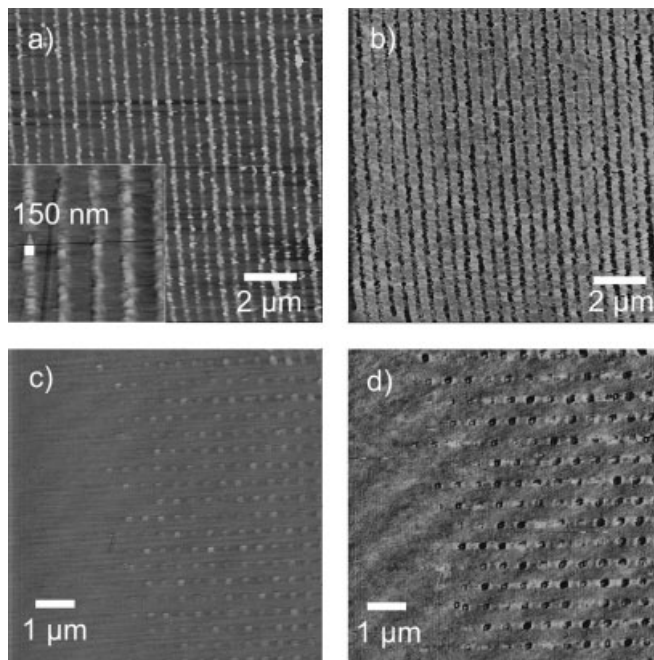
Figure 3. Contact-mode height (a,c) and friction (b,d) AFM images of fluoroalkyl SAM lines (a,b) and dots (c,d). The lines are 150 nm wide at a period of 500 nm, while the dots are 125 nm in diameter with a period of 500 nm. Brighter areas in the friction images indicate higher friction.

tion (Figs. 3b,d) images of an array of fluoroalkyl SAM lines of about 150 nm width at a period of 500 nm (Figs. 3a,b) as well as an array of dots of about 125 nm diameter at a period of 500 nm (Figs. 3c,d). It shows that this process still works for creating silane SAM patterns with dimensions close to 100 nm. The observed edge roughness of several tens of nanometers can be attributed not only to the process (mainly to the quality of the stamp, but possibly also to non-optimized imprint parameters and the isotropic residual-layer removal), but also to the difficulty of imaging such samples using AFM.

XPS imaging of fluoroalkyl SAMs patterned by NIL (Fig. 4) showed the presence of fluorine only in the areas imprinted by NIL and thus free for SAM formation. Partial spectra of F_{1s} and C_{1s} (not shown) in and outside the squares prove the selec-
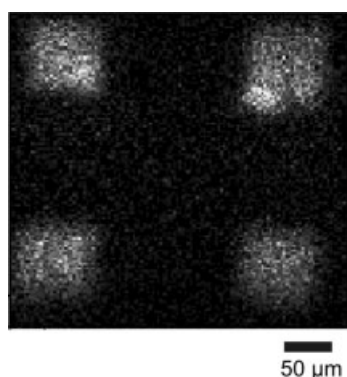
Figure 4. XPS F mapping of 100 μm fluorinated SAM squares and partial spectra made inside and outside a square. The sample was prepared by imprinting an array of squares followed by residual-layer removal. A fluor-oalkylsilane was evaporated on the sample and the polymer was completely removed in acetone using ultrasound.

tivity of the SAM formation process because they show the presence of F and C–F peaks respectively in the squares while they are absent outside them. Thus, these results confirm that SAM formation occurred exclusively in the NIL-patterned areas.

NIL-patterned SAMs after polymer removal were subjected to evaporation of a second silane adsorbate (Scheme 1, path A). As a result, the substrate was chemically patterned with two different kinds of SAMs. Figure 5 shows height (Fig. 5a) and friction (Fig. 5b) AFM images of a sample patterned with an alkyl SAM. Shown in the same Figure are the height (Fig. 5c) and friction (Fig. 5d) AFM images of the same sample after subsequent formation of an aminoalkyl SAM in the remaining free areas. For the first silanation, a higher friction force was observed on the substrate than on the alkyl SAM. After the second silanation, the friction was higher on the aminoalkyl SAM than on the alkyl SAM, in agreement with the hydrophilic degree of the respective SAMs (see Table 1). Evaporation of the aminoalkyl silane on the 150 nm fluoroalkyl SAM lines and 125 nm dots (see Fig. 3) led to similar results. Assuming that gas-phase adsorption of silanes is not limited by the size of the imprinted features, the resolution of
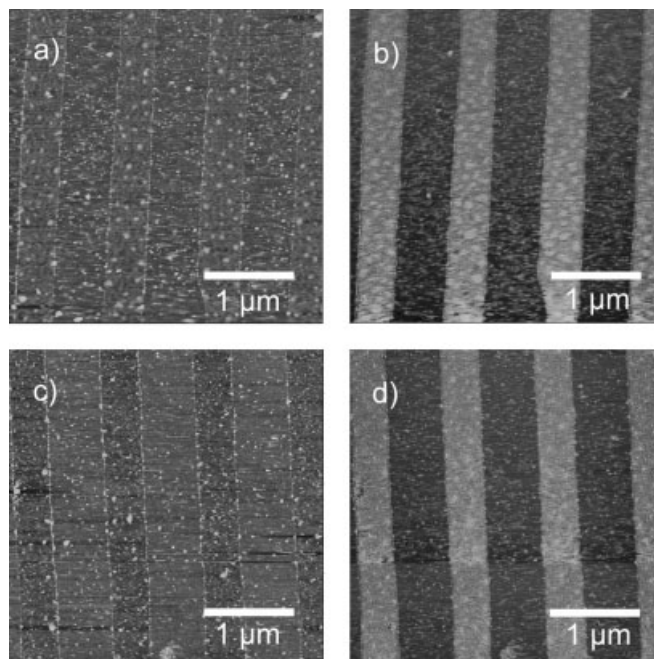

Figure 5. Contact-mode height (a,c) and friction (b,d) AFM images of a substrate patterned with 600 nm alkyl SAM lines at 1 μm period, made using NIL (a,b), and after subsequent evaporation of an aminoalkylsilane (c,d).

SAM patterning using NIL is thus only limited by the resolution of NIL itself.

## 2.2. Deposition of Nanoparticles on NIL-Patterned SAMs

Carboxylate-functionalized nanoparticles were chosen for electrostatic attachment on the aminoalkyl SAMs after protonation. Protonation of the aminoalkyl monolayer was performed by rinsing the sample with a 4-morphilineethanesulfonic acid monohydrate (MES) buffer (pH 5.6). Two kinds of functionalized particles were attached by drop casting: i) 50 nm silica particles functionalized with carboxylic acid groups,[28] and ii) 350 nm commercial polystyrene (PS) beads functionalized with carboxylic acid groups.

Particles were adsorbed on NIL-patterned aminoalkyl SAMs without removal of the polymer. The polymer behaves then as a physical barrier to prevent the deposition of particles on the protected areas (see Scheme 1, path B). Figure 6 shows scanning electron microscopy (SEM) images of carboxylate-functionalized 350 nm PS beads attached to an aminoalkyl SAM formed on a NIL-patterned substrate. The PS beads attached preferentially to the aminoalkyl SAM. In Figure 6a, the ordered PS beads indicate that wetting of the pattern by the suspension is not a problem, as the particles show the characteristic zigzag arrangements caused by a line width between d and $2d$ (where d is the diameter of the particles).[29] In Figure 6b, the ordered and packed beads seem to center at the SAM line. This is probably due to the process of drying under N_2 flow.
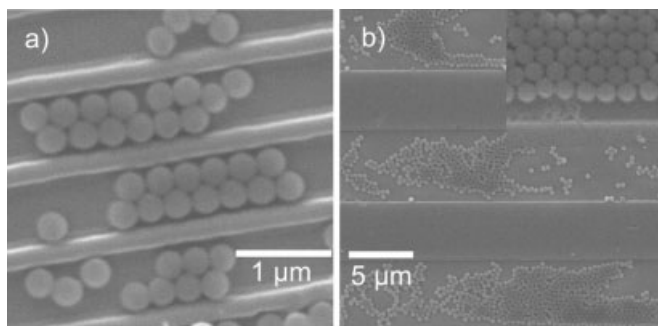
Figure 6. SEM images of 350 nm carboxylate-functionalized PS beads adsorbed to the 700 nm (a) and 5 μm (b) aminoalkyl SAM lines prepared by NIL followed by silane adsorption. Inset: a close-up showing close-packed PS beads.

Figures 7a,b show SEM images of silica particles attached to the aminoalkyl SAM areas of a NIL-patterned sample, after subsequent removal of the polymer. This was not attempted for PS beads, since PS beads may dissolve in acetone while the mask is being removed. When silica particles were used, the
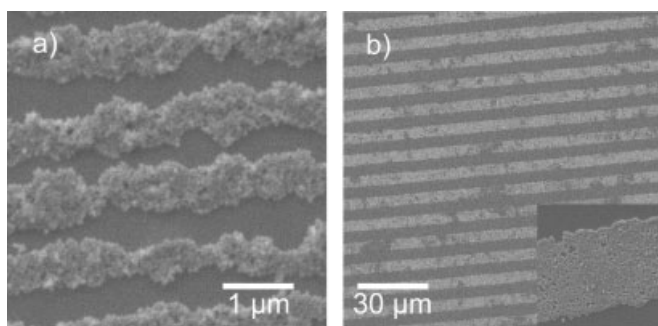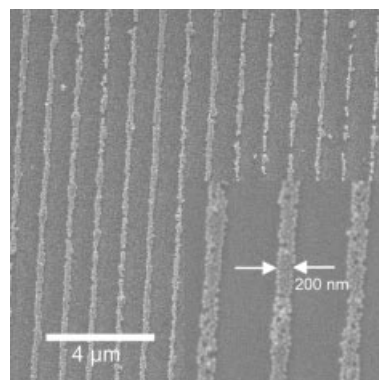

Figure 7. SEM images of 50 nm carboxylate-functionalized silica particles adsorbed to 700 nm (a) and 5 μm (b) aminoalkyl SAM lines, the polymer template was removed afterwards. The inset shows a close-up of close-packed silica particles.

polymer template could be removed in acetone because silica particles do not dissolve in acetone. Comparison with SEM pictures made before polymer removal (not shown) showed no damage to the particle pattern. Dense packing of the particles was observed for all patterns, independent of the linewidth. Places initially covered by the polymer were found to be free of particles. However, the edges of the patterns are not well defined owing to the drying phenomena, as described above.

The advantage of our process is that the chemical SAM pattern allows for attachment of particles, and possibly also molecules and proteins, onto the SAM areas while the polymer template masks the remainder of the surface. This method can be compared to template-assisted self-assembly (TASA)[30,31] that uses a template to assemble monodispersed colloids into organized structures by capillary forces. The difference is that in our case, the particles are electrostatically attached to the monolayer and thus the template can be removed after attachment of the particles. Another advantage is that a second

monolayer can then be formed on the substrate and attachment of, e.g., another kind of particle can be performed.

Alternatively, particle adsorption was performed on substrates patterned with two adsorbates (Scheme 1, path A). As described above, an alkyl SAM was formed on a NIL-patterned substrate followed by polymer removal. Increasing the immersion time in acetone, while removing the residual layer, allowed one to reduce the width of the polymer lines obtained after NIL. After complete removal of the polymer, a second adsorbate, an aminoalkyl SAM, was attached to the areas previously protected by polymer. Finally, carboxylate-functionalized particles were electrostatically attached to the sample (See Scheme 1, path A). Figure 8 shows a SEM image of carboxylate-functionalized silica particles attached to the aminoalkyl SAM areas, which are in this case only 200 nm wide. The parts corresponding to the alkyl SAM appear clean of par-

Figure 8. SEM image of 50 nm carboxylate-functionalized silica particles adsorbed to a NIL-patterned aminoalkyl SAM (300 nm wide lines), the complementary pattern (700 nm wide lines) corresponding to an alkyl SAM region. Inset: a close-up of a close-packed area.

ticles. Carboxylate-functionalized silica particles were densely packed and matched closely the dimension of the aminoalkyl SAM areas, as it can be noted that the edges of the lines are relatively well defined. A height of 50 nm was measured using AFM, which corresponds to a monolayer of particles. Close-packed particles can be observed in the inset of Figure 8. Additionally, carboxylate-functionalized 350 nm PS beads were used and selective attachment on the aminoalkyl SAM was observed as well (images not shown). CF_3- and CH_3-terminated monolayers showed the same properties with respect to attachment of particles. Namely, particle attachment on CF_3/NH_3^+-terminated SAMs was found to be as selective as on CH_3/NH_3^+-terminated SAM patterns. The selectivity of particle attachment also did not change with pattern sizes. High selectivity was obtained for both silica particles and PS beads, as no particles can be seen on the alkyl SAM parts. The main advantages of the chemical patterning over the usual template patterning of arrays of particles are that the liquid can wet the pattern very well, as there are no physical barriers to prevent it and there is no risk of introducing disorder in the array of particles while removing the template.

2.3. Towards Molecular Devices

NIL-patterned substrates are three-dimensional, in contrast to the pseudo-two-dimensional nature of a patterned SAM. One of the advantages of using NIL to pattern SAMs is that the remaining patterned polymer can be used for additional microelectronic processes such as metal lift-off. In order to demonstrate the feasibility of this process (Scheme 1, path C), an aminoalkyl monolayer was formed on an imprint and a 10 nm thick layer of gold was evaporated on top. The polymer was removed in acetone using ultrasound. Figure 9a shows an AFM image of gold lines obtained via this process. The metal sticks well to the top of the monolayer after lift-off, and can be used later as a top-electrode. A line thickness of 12 nm was extracted from the height profile of the AFM image and this corresponds to the thickness of the evaporated gold.

Thereafter, the gold layer was etched using a wet-etching solution. Figures 9b,c show the same sample as in Figure 9a, after 6 min in a solution of $Na_2S_2O_3$ (0.1 M), KOH (1.0 M), $K_3Fe(CN)_6$ (10 mM), and $K_4Fe(CN)_6$ (10 mM). The 800 nm width of the aminoalkyl SAM is retained, in height (Fig. 9b) as well as in friction (Fig. 9c). This suggests that the monolayer remains after gold evaporation and lift-off. This experiment shows that an aminoalkyl SAM can be an alternative to the commonly used titanium adhesion layer to deposit gold on silicon oxide. This technique can be employed in the fabrication of hybrid electronic devices such as organic field-effect transistors (OFETs) because the use of a titanium adhesion layer generally diminishes the injected current from the metal contacts to the organic semiconductor layer at the substrate interface where charge transport takes place.[32] Additionally, a simplified fabrication procedure can be achieved considering that a silane monolayer is generally grown on the substrate in the region between the contacts to make the organic semiconductor compatible with the inorganic substrate.[33] The experiment also shows that molecular electronic devices can be made by multiprocessing, i.e., combining self-assembly and NIL, when using SAMs containing functional groups.

3. Conclusions

We have shown that NIL is a soft-lithography method that can be used for chemical patterning silicon oxide substrates with a single monolayer as well as binary monolayers. A large range of monolayers with different end groups can be used. This method allows one to pattern with a high resolution over large areas. Here, we have demonstrated patterns close to 100 nm, which would be very difficult and/or very expensive to produce otherwise.

We have shown initial results in the use of such patterns in nanoparticle deposition. Both substrates with the polymer patterns still maintained and substrates with binary SAMs have been employed. Whereas the polymer patterns of the former can function as physical barriers resisting adsorption while the SAM directs the adsorption to the complementary areas, it is clear that drop-casting causes imperfect particle patterns, although this could potentially be solved using other deposition strategies. Nevertheless, the advantage of using a functional SAM to direct the particle deposition is clearly shown by the fact that the polymer can be removed afterwards while retaining the particle assemblies. In contrast, the binary SAM samples have the advantage of eliminating such wetting problems. The potential of using SAMs is shown here even more powerful, as the deposition selectivity can be close to perfect.

Thus, this rather simple stepwise process allows for the fabrication of sub-micrometer chemical patterns, which can be either followed by metal lift-off, or can be used as a base for the selective attachment of sub-micrometer functionalized particles by drop-casting. The accurate control of the position of particles at the sub-micrometer range can potentially be applied to chemical studies of specific interactions between SAM and nanoparticle interfaces, to photonic crystals, and to memory devices. Further investigations into the limiting resolution of the method and into the preparation of more densely packed and better-ordered particle arrays are currently in progress.
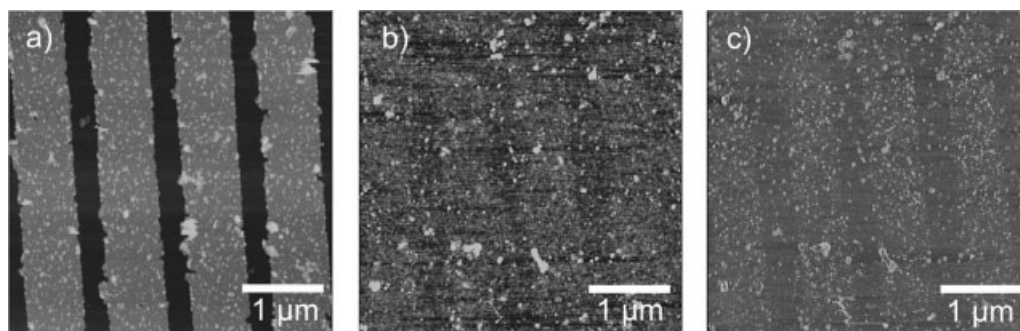
Figure 9. Contact-mode height (a,b) and friction (c) AFM images of 800 nm lines prepared by NIL and evaporation of an aminoalkyl silane in the vacant areas, followed by evaporation of a 10 nm thick film of Au and the subsequent removal of the polymer in acetone and ultrasound before (a) and after (b,c) wet-etching of the gold layer.

4. Experimental

Compounds: 1*H*,1*H*,2*H*,2*H*-perfluorodecyltrichlorosilane, dodecyltriethoxysilane (from ABCR), *N*-[3-(trimethoxysilyl)propyl]ethylenediamine (Aldrich), dodecyltrichlorosilane (Acros), bromoundecyltrichlorosilane (Gelest), and PMMA (weight-average molecular weight, M_W 350 kD, Aldrich) were used. Carboxylate-functionalized PS beads in aqueous suspension (350 nm diameter) were obtained from Polyscience Inc. Fabrication of carboxylate-functionalized 50 nm silica particles has been described elsewhere [28].

Analysis: The quality and reproducibility of the gas-phase evaporation were investigated by water-contact-angle goniometry, ellipsometry, AFM, and XPS. Water-contact-angle measurements and ellipsometry were performed on a large number of samples, before and after ultrasound of duration 20 min. Contact angles were determined using a Krüss Contact Angle Measurement System G 10, and the data processed with the program Drop Shape Analysis 1.51. In the case of unpatterned films, the monolayer thickness was measured by opening a trench on the monolayer by means of the AFM tip. Quantitative surface elemental analysis and spatial localization were performed. XPS was performed on patterned SAM using a PHI Quantera Scanning ESCA Microprobe.

Samples were investigated using an atomic force microscope AFM Nanoscope III (Veeco, Digital Instruments, USA) in contact mode and equipped with a Si_3N_4 tip with a J scanner operating at a scan rate of 1.5 Hz. SEM investigation was performed with a JEOL 5610 apparatus. In the case of the attachment of PS beads, the sample were covered with 5 nm of Au to facilitate SEM observation.

NIL: The stamps were made by photolithography followed by reactive-ion etching (RIE, Elektrotech Twin system PF 340) or by EBL followed by titanium evaporation and lift-off. They consisted of gratings composed of 400 nm wide lines at a 1 μm period, 5 μm lines at a 10 μm period, or 5 μm lines at a 15 μm period with a height of 300 nm. A second type of stamps contained 150 nm wide lines at a period of 500 nm and 125 nm dots at a period of 500 nm with a height of 85 nm. 1*H*,1*H*,2*H*,2*H*-perfluorodecyltrichlorosilane was used as an anti-adherent layer to facilitate the stamp–imprint separation. Silicon substrates were oxidized first by immersion in piranha solution (concentrated H_2SO_4 and 33 % aqueous H_2O_2 in a 3:1 ratio. *Warning*: piranha solution should be handled with caution; it is known to detonate unexpectedly) for 15 min (SiO_x thickness 1.5 nm) and then covered with a 400 nm thick layer of PMMA by spin-coating. Stamp and substrate were put in contact and a pressure of 40 bar was applied at a temperature of 180 °C using a hydraulic press (Specac). The residual layer was removed by dipping the samples in acetone during 60 s or by O_2 plasma during 20 s using a RIE system. The imprints consisted then in 10 μm polymer lines at a 15 μm period, 5 μm polymer lines at a 10 μm, and 600 nm polymer lines at a 1 μm period. When necessary, the polymer template was removed in acetone and ultrasound over 2 h. The imprint cycle time was 20 min and the imprinted area was 2 cm × 2 cm. The stamps were changed approximately every fifty imprints.

SAM Formation: The gas-phase evaporation of silanes was performed in a desiccator under vacuum. The samples were left several hours or overnight and then carefully rinsed with ethanol and Millipore water.

Nanofabrication: Samples were rinsed with MES, pH 5.6 buffer. Particle attachment was performed using a suspension of either 50 nm carboxylated silica particles or 350 nm carboxylated PS beads. Attachment was performed by casting a drop of the suspension on the substrate and leaving it to dry for 1 h. Samples were placed in a standing position in the suspension to avoid non-specific interactions induced by gravity. Samples were then copiously rinsed with high-purity water and carefully dried in a N_2 flow.

A 10 nm layer of gold was evaporated using a metal evaporator BAK 600 in a vacuum of 1×10^{-6} mbar. The metal lift-off was carried out in acetone and ultrasound. For the wet-etching of gold, the sample was immersed for 6 min in gold wet-etchant solution ($Na_2S_2O_3$ (0.1 M), KOH (1.0 M), $K_3Fe(CN)_6$ (10 mM), and $K_4Fe(CN)_6$ (10 mM); etching rate: ~ 3 nm min^{-1}).

[1] B. Michel, A. Bernard, A. Bietsch, E. Delamarche, M. Geissler, D. Juncker, H. Kind, J. P. Renault, H. Rothuizen, H. Schmid, P. Schmidt-Winkel, R. Stutz, H. Wolf, *IBM J. Res. Dev.* **2001**, 45, 870.

[2] N. Abbot, A. Kumar, G. M. Whitesides, *Chem. Mater.* **1994**, 6, 596.

[3] N. J. van der Veen, S. Flink, M. A. Deij, R. J. M. Egberink, F. C. J. M. van Veggel, D. N. Reinhoudt, *J. Am. Chem. Soc.* **2000**, 122, 6112.

[4] C. Zhou, M. R. Deshpande, M. A. Reed, *Appl. Phys. Lett* **1997**, 71, 611.

[5] Y. Chen, D. A. Ohlberg, X. Li, D. R. Stewart, J. O. Jeppesen, K. A. Nielsen, J. F. Stoddart, D. L. Olynick, E. Anderson, *Appl. Phys. Lett.* **2003**, 82, 1610.

[6] H. Zhu, M. Snyder, *Curr. Opin. Chem. Biol.* **2003**, 7, 55.

[7] G. Kaltenpoth, M. Himmelhaus, L. Slansky, F. Caruso, M. Grunze, *Adv. Mater.* **2003**, 15, 1113.

[8] I. Lee, H. Zheng, M. F. Rubner, P. T. Hammond, *Adv. Mater.* **2002**, 14, 572.

[9] V. Santhanam, R. P. Andres, *Nano Lett.* **2003**, 4, 41.

[10] T. Auletta, B. Dordi, A. Mulder, A. Sartori, S. Onclin, C. M. Bruinink, M. Péter, C. A. Nijhuis, H. Beijleveld, H. Schönherr, G. J. Vancso, A. Casnati, R. Ungaro, B. J. Ravoo, J. Huskens, D. N. Reinhoudt, *Angew. Chem. Int. Ed.* **2004**, 43, 369.

[11] C. A. Fustin, G. Glasser, H. W. Spiess, U. Jonas, *Adv. Mater.* **2003**, 15, 1025.

[12] Y. Masuda, M. Itoh, T. Yonezawa, K. Koumoto, *Langmuir* **2002**, 18, 4155.

[13] Y. Xia, Y. Yin, Y. Lu, J. McLellan, *Adv. Funct. Mater.* **2003**, 13, 907.

[14] Y. Xia, G. M. Whitesides, *Angew. Chem. Int. Ed.* **1998**, 37, 550.

[15] R. D. Piner, J. Zhu, F. Xu, S. Hong, C. A. Mirkin, *Science* **1999**, 283, 661.

[16] A. Pallandre, K. Glinel, A. M. Jonas, B. Nystem, *Nano Lett.* **2004**, 4, 365.

[17] A. Golzhauser, W. Eck, W. Geyer, V. Stadler, T. Weimann, P. Hinze, M. Grunze, *Adv. Mater.* **2001**, 13, 806.

[18] S. Y. Chou, P. R. Krauss, P. J. Renstrom, *Science* **1996**, 272, 85.

[19] S. Y. Chou, P. R. Kraus, *Microelectron. Eng.* **1997**, 35, 237.

[20] C. M. Sotomayor Torres, *Alternative Lithography*, Kluwer, Dordrecht, The Netherlands **2004**.

[21] W. Wu, J. Gu, H. Ge, C. Keimel, S. Y. Chou, *Appl. Phys. Lett.* **2003**, 83, 2268.

[22] Z. Yu, P. Deshpande, W. Wu, J. Wang, S. Y. Chou, *Appl. Phys. Lett.* **2000**, 77, 927.

[23] G. D. Bachand, R. K. Soong, H. P. Neves, A. Olkhovets, H. G. Craighead, C. D. Montemagno, *Nano Lett.* **2001**, 1, 42.

[24] M. D. Austin, S. Y. Chou, *Nano Lett.* **2003**, 3, 1687.

[25] When the immersion time in acetone was extended, the lateral dissolution of PMMA produced a reduction of the width of the polymer lines (e.g., from 600 nm to 200 nm in 90 s).

[26] C. H. Chen, J. P. Ibbetson, E. L. Hu, U. K. Mishra, *Appl. Phys. Lett.* **1997**, 71, 494.

[27] A. Szekeres, S. Alexandrova, K. Kirov, *Phys. Status Solidi* **1980**, 62, 727.

[28] V. Mahalingam, S. Onclin, M. Péter, B. J. Ravoo, J. Huskens, D. N. Reinhoudt, *Langmuir* **2004**, 20, 11756.

[29] Y. Xia, Y. Yin, Y. Lu, J. McLellan, *Adv. Funct. Mater.* **2003**, 13, 907.

[30] Z.-Z. Gu, A. Fujishima, O. Sato, *Chem. Mater.* **2002**, 14, 760.

[31] Y. Yin, Y. Xia, *J. Am. Chem. Soc.* **2001**, 123, 771.

[32] R. A. Street, A. Salleo, *Appl. Phys. Lett.* **2002**, 81, 2887.

[33] Charge injection through metal–organic semiconductor junctions is determined by the energy difference between the work function of the metal and the relevant molecular orbital of the semiconductor (highest occupied molecular orbital (HOMO) or lowest unoccupied molecular orbital (LUMO)) both measured relative to the vacuum level. Most of the stable organic semiconductors reported in the literature are p-type and the HOMO level (e.g., pentacene, activation energy + energy gap = 5.1 eV) for most of them aligns well with the Fermi level of gold (work function = 5.1 eV) leading to the formation of ohmic contacts for hole injection. In contrast, Ti leads to the formation of an energy barrier and the electrodes block injection of holes. T. Li, J. W. Balk, P. P. Ruden; I. H. Campbell, D. L. Smith, *J. Appl. Phys.* **2002**, 91, 4312.